

Article

Braneworld Inspires Cosmological Implications of Barrow Holographic Dark Energy

Shamaila Rani * and **Nadeem Azhar**

Department of Mathematics, Lahore-Campus, COMSATS University Islamabad, Lahore 54000, Pakistan; nadeemazharsaeed@gmail.com

* Correspondence: drshamailarani@cuilahore.edu.pk

Abstract: In the present manuscript, the evolution of the cosmic parameters and planes are being investigated in the framework of the DGP braneworld model. In this scenario, the interaction Γ between the Barrow holographic dark energy model (whose infrared cutoff scale is set by Hubble and event horizons) and pressureless dark matter are considered. We check the behavior of different cosmological parameters such as Hubble, equation of state, deceleration and squared speed of sound from the early matter-dominated era until the late-time acceleration. It is found that the range of Hubble parameter lies in the interval 95_{-35}^{+35} (for Hubble horizon) and 97_{-23}^{+23} (for event horizon). For both horizons, the equation of state parameter favors the phantom dominant era as well as the Λ CDM model while the deceleration parameter illustrates the accelerated expansion of the universe. Furthermore, stability of the underlying model is found through squared speed of sound. Furthermore, it is observed that $\omega - \omega'_\theta$ plane corresponds to freezing and thawing region for Hubble and event horizons, respectively. Furthermore, statefinder plane shows the Λ CDM and Chaplygin gas behavior for both models. Finally, we investigate the thermodynamical nature of the underlying model through Barrow entropy as horizon entropy and found validity for both horizons.



Citation: Rani, S.; Azhar, N. Braneworld Inspires Cosmological Implications of Barrow Holographic Dark Energy. *Universe* **2021**, *7*, 268. <https://doi.org/10.3390/universe7080268>

Academic Editor: Stefano Bellucci

Received: 26 May 2021

Accepted: 18 July 2021

Published: 27 July 2021

Publisher's Note: MDPI stays neutral with regard to jurisdictional claims in published maps and institutional affiliations.



Copyright: © 2021 by the authors. Licensee MDPI, Basel, Switzerland. This article is an open access article distributed under the terms and conditions of the Creative Commons Attribution (CC BY) license (<https://creativecommons.org/licenses/by/4.0/>).

1. Introduction

The universe is expanding, a well-established fact based on studies of type Supernova *Ia* (SNe Ia) [1,2], gravitational lensing (GL) [3], cosmic microwave background radiation (CMBR) [4,5] and the baryonic acoustic oscillations (BAO) [6,7]. It is strongly suggested that this type of expansion is attributed to an unknown force called dark energy (DE) [8–13]. The only known property of DE can be described as a fluid having negative pressure (repulsive force), which accounts for 76% of the total energy density of the current universe. The Λ CDM model (Λ) was the first model to investigate DE, whose equation of state is constant ($\omega_\theta = -1$), but it dubbed two basic problems, named fine-tuning [14–18] and cosmic coincidence problems [7]. A large number of theoretical DE models and modified theories of gravity have been proposed in the literature to describe the possible existence of DE. Some promising DE models are pilgrim DE model [19–21], K-essence [22–24], new agegraphic DE model [25,26], holographic DE (HDE) model [27,28] and its modified families. Similarly, on orientation of the modified theories of gravity, there are many attempts, for instance, the $f(R)$ gravity (where R denotes the Ricci scalar) [29,30], $f(T)$ gravity (where T expresses the torsion scalar) [31], $f(G)$ gravity (where G presents the Gauss–Bonnet term) [32,33], the Dvali–Gabadadze–Porrati (DGP) braneworld model [34] and so on.

According to the braneworld scenario, our universe is realized as a 3-brane embedded in a higher-dimensional spacetime. One of the new versions of the braneworld scenario is proposed by DGP, which states as our four-dimensional Friedmann–Robertson–Walker (FRW) universe embedded in five-dimensional Minkowski spacetime. In this context, the

usual gravitational laws are recovered by adding the action of brane (computed with the brane intrinsic curvature) with Einstein–Hilbert action. The DGP model has two main forms of solutions, the first one is the self-accelerating form while other is the normal form. The first form of DGP model explores the late-time cosmic acceleration without recourse to DE [35,36]. Unfortunately, this form of DGP has ghost instabilities and it cannot realize a phantom divide crossing by itself, so it is necessary to add at least a component of energy to obtain a phantom-like phase. On the other hand, the normal form of the DGP model can realize a phantom-like phase, but cannot describe the accelerated expansion of the universe. Therefore, by adding a DE component to the normal form, one can explain late-time acceleration with new facilities which also shown good consistency with observations. In the literature, a lot of authors have considered the DGP model to explore different cosmological issues. Mukherjee [37] investigated the spherical collapse of matter overdensity by using the semi-analytic approach in the context of the DGP braneworld model. The structure formation [38], growth of large scale structure [39] and numerical study of cosmological perturbation [40] are studied in braneworld cosmology. Biswas et al. [41] investigated various physical aspects of the generalized ghost DE model in the context of braneworld cosmology. They studied cosmological parameters (Hubble, equation of state, deceleration, Adiabatic sound speed), planes ($\omega_\theta - \omega'_\theta$, state-finder) and found a stable solution that is consistent with observational datasets.

Description of DE through the well-known holographic principle (HP) (the entropy of black hole is proportionate to its area) has become an interesting approach at cosmological framework. The HDE model was the first attempt which is not only the best candidate to describe DE but also in agreement with observational data. One can obtain the vacuum energy density of the HDE model due to the connection between ultra-violet (UV) cutoff (short distance cutoff) and infra-red (IR) cutoff (largest length of quantum field theory). Initially, Li derived its energy density as $\rho_\theta = 3n^2 M_{pl}^2 L^{-2}$, where n denotes the numerical constant, $M_{pl} = \frac{1}{\sqrt{8\pi G}}$ is the reduced Planck mass and L expresses the horizon of the universe. Inflationary evolution of the universe in the context of the HDE model is studied in [42–47] while Gao et al. [48] investigated HDE model with Ricci scalar curvature. In addition to all of these achievements, the minimal HDE model has a number of problems. The biggest problem is that the χ^2 is higher than flat Λ CDM even through HDE has an extra parameter. This appears to be down to an incompatibility with observational data within HDE [49]. Furthermore, the minimal HDE model with Hubble horizon is not a good choice, since it precludes DE [27]. Furthermore, some new types of HDE model are modified by utilizing different generalized entropies with holographic fundamentals. These extended forms are the Tsallis HDE model [50], the Renyi HDE model [51,52], the SharmaMittal HDE model [53,54] and the barrow HDE model [55]. These modified HDE models are obtained by utilizing HP with different generalized entropies.

The entropy is the essential concept to explore universal features of a system from its microscopic details. The Bekenstein–Hawking entropy (black hole entropy) [56,57] is a non-extensive quantity, proportional to the area of its event horizon A defined as $S_{BH} = \frac{A}{4}$. From the statistical point of view, Boltzmann and Gibbs has initially defined as entropy in terms of the probability distribution. Gibbs entropy is defined over an ensemble while Boltzmann thought the entropy is the macroscopic state of a system. In modern physics, Boltzmann–Gibbs (BG) entropy which is motivated by statistical physics, is known as the basic entropy. The BG entropy is further generalized in a dynamical system, information theory and statistical physics. Kolmogorov–Sinai entropy [58] is an example of generalized entropy related to the dynamical system while Rényi entropy is an example of information theory. Another important generalization of standard BG entropy is Tsallis non-extensive entropy constructed by Tsallis and Cirto [50]. In [59], Tsallis argued that BG entropy would not be a suitable entropy to describe a black hole (BH) as this entropy is not proportional to the BH volume. In 1975, Sharma and Mittal constructed another form of generalized entropy named Sharma–Mittal (SM) entropy [60]. Some remarkable features of SM entropy

are that it fails to be concave [61] (requires thermodynamical stability) and it is not Lasche-stable [62] (stability for small variations of the probabilities).

Recently, Barrow [63] proposed a new form of entropy inspired by COVID-19 virus cases, named Barrow entropy. This entropy is a quantum gravitationally corrected black-hole entropy due to the fractal structure brought about in its horizon. Mathematical form of Barrow entropy is considered as

$$S_B = \left(\frac{A}{A_0} \right)^{1+\frac{\Delta}{2}}, \quad (1)$$

where A and A_0 are the normal and Planck area, respectively, while Δ denotes the quantum deformation. The maximal deformation exist for $\Delta = 1$ while for $\Delta = 0$ we recover normal (Bekenstein) entropy. Next, Saridakis [55] derived the Barrow HDE (BHDE) model by utilized the HP in a cosmological structure and Barrow entropy. The energy density of this BHDE model is defined as

$$\rho_\theta = CL^{2-\Delta}, \quad (2)$$

where the parameter C has the dimension $[L^{-2-\Delta}]$. In literature, various IR cutoffs have been proposed to understand the dynamics of universe. In this paper, we consider the Hubble ($L = \frac{1}{H}$) and the event $(L = R_h = a(t) \int_t^\infty \frac{dt}{a(t)})$ horizons as IR cutoffs. Motivation of these cutoffs are as follows.

In case of event horizon, we found some difficulty as there does not exist any standard big bang model against this horizon. Furthermore, for the accelerating era of the universe, the event and Hubble horizons have different forms. Wang et al. [64] checked the validity of thermodynamics laws (first and second thermodynamics laws) for Hubble and event horizon with Bekenstein entropy as horizon entropy. They considered the usual definition of the temperature and entropy and found compatibility for Hubble horizon while the violation of these laws are obtained in case of the event horizon. They demonstrated that the event horizon presented the global space-time properties; therefore, it is larger than Hubble horizon. They argued that this horizon universe remains non-static and, therefore, thermodynamical quantities are different and not as simple as in static space-time. Sadjadi and Honardoost [65] considered the linear combination of Hubble and event horizon in the framework of the interacting HDE model and investigated the possibility of crossing $\omega = -1$ by assuming the validity of second thermodynamical law. Arevalo et al. [66] checked the validity of the generalized second law of thermodynamics (GSLT) for Hubble, event and linear combination of these horizons. They also considered the interacting HDE model in a FRW background and found constraints, under which the generalized second law is valid.

Many authors studied remarkable works in the framework of the BHDE model. Archana et al. [67] explored statefinder diagnostic for a flat FRW universe in the framework of the BHDE model. Sharma et al. [68] studied a Barrow agegraphic DE model and found the nature of some cosmological parameters and planes. Similarly, Srivastava and Sharma [69] investigated the evolutionary history of cosmological parameters and reconstructed the quintessence scalar field model for the BHDE model with Hubble cutoff. Mamon et al. [70] proposed an interacting model of BHDE and discussed cosmological parameters and planes as well as the generalized second law of thermodynamics for a spatially flat FLRW universe. In this manuscript, we investigate the nature of some cosmological parameters (Hubble, equation of state, deceleration, squared speed of sound) and planes ($\omega_\theta - \omega'_\theta$, statefinder) for the BHDE model with Hubble and event horizon under DGP cosmology. We also present the graphical behavior of each parameter and plane and found stable solutions. We also check the stability of the underlying model through the generalized second law of thermodynamics. The structure of this paper is as follows. In the next section, we discuss the field equations of DGP braneworld cosmology. Section 4 is dedicated to investigating the dynamics of cosmological parameters. In Section 5, we extend our study towards cosmological planes. The generalized second law

thermodynamics is studied in Section 6. Finally, the last section is devoted to a summary of our results.

2. Field Equation

We consider a homogeneous and isotropic FRW universe on the brane which can be described by the line element

$$ds^2 = -dt^2 + a^2(t) \left(\frac{dr^2}{1 - kr^2} + r^2 d\Omega^2 \right), \quad (3)$$

where $a(t)$ and k are the scale factor and curvature parameter. The open, flat and closed universe can be characterized for $k = -1, 0, 1$, respectively. For a flat FRW universe, the modified Friedmann equation in DGP braneworld cosmology [35] is given by

$$H^2 = \left(\sqrt{\frac{\rho}{3M_p^2} + \frac{1}{4r_c^2}} + \frac{\epsilon}{2r_c} \right)^2, \quad (4)$$

where $H(a)$ is a Hubble parameter such that $H(a) = \frac{\dot{a}}{a}$ and dot presents its derivative with respect to (w.r.t) time t . The crossover length scale is denoted by r_c such that $r_c = \frac{M_p^2}{2M_5^3} = \frac{G_5}{2G_4}$, it is also interesting to mention here that $\frac{1}{H} \ll r_c$ corresponds to 4D general relativity and the contradiction leads to significant effect of 5D. Furthermore, $\rho = \rho_\theta + \rho_m$, where ρ_θ and ρ_m are the energy densities of DE and dark matter (DM), respectively, M_p is reduce Planck mass and $\epsilon = \pm 1$. This value of ϵ leads to two types of solutions of the DGP cosmology, first one is self accelerating solution ($\epsilon = +1$) and the second one presents normal branch ($\epsilon = -1$). The normal branch is shown as the accelerating phase of the universe due to the DE component while the self accelerating branch expresses acceleration without the presence of an additional DE component. In standard cosmology, Equation (4) can also be written as

$$H^2 - \frac{\epsilon}{r_c} H = \frac{\rho}{3M_p^2}. \quad (5)$$

The above equation can also be written in fractional energy density form by considering $\Omega_m = \frac{\rho_m}{3M_p^2 H^2}$, $\Omega_\theta = \frac{\rho_\theta}{3M_p^2 H^2}$ and $\Omega_{rc} = \frac{1}{4H_0^2 r_c^2}$ (where H_0 denotes the present value of Hubble parameter). Therefore, Equation (5) in the form of fractional density becomes

$$1 = \frac{2\epsilon H_0}{H} \sqrt{\Omega_{rc}} + \Omega_m + \Omega_\theta \Rightarrow 1 = \Omega_B + \Omega_m + \Omega_\theta, \quad (6)$$

where $\Omega_B = \frac{2\epsilon H_0}{H} \sqrt{\Omega_{rc}}$. In further calculations, we consider $M_p^2 = 1$. In this manuscript, we are assuming non-interaction conservation equations between DE and DM that leads to the following form

$$\dot{\rho}_\theta + 3H(\rho_\theta + p_\theta) = -\Gamma, \quad (7)$$

$$\dot{\rho}_m + 3H(\rho_m + p_m) = \Gamma, \quad (8)$$

where Γ is the interaction term that presents the rate of energy exchange between dark sectors. From conservation Equation (7), it clear that $\Gamma < 0$ corresponds to the energy transfer from DM to BHDE while $\Gamma > 0$ shows the energy transfer from BHDE to DM. The non-interaction case ($\Gamma = 0$) leads energy density of DE as $\rho_m \propto a^{-3}$. Therefore, the non-interaction case is more general to understanding the dynamics of the universe with different perspectives. In the literature [71], many linear and non-linear interaction terms have been proposed, which are the function of ρ_θ , ρ_m and H and their linear combinations. Among these interaction terms, $\Gamma = 3Hd^2\rho_m$ is most effective case [72]. Hence, In this

work, we consider $\Gamma = 3Hd^2\rho_m$ (where d^2 is the coupling constant). Using this choice of Γ in Equation (8), we have

$$\rho_m = \rho_{m0}a^{3(d^2-1)}, \quad (9)$$

where ρ_{m0} is the integration constant.

3. Cosmological Parameters and Planes

In this section, we briefly discuss some basic but important cosmological parameters like Hubble (H), EoS (ω_θ), deceleration (q) and squared speed of sound (V_s^2). The most important feature of these parameters are that they not only describe the formation of the universe from neutrinos, baryons, dark matter and DE but also tell us about the global dynamics of the universe such as expansion rate and curvature. Hence, we investigate these feature of the universe through above mention parameters for BHDE model in the framework of DGP braneworld cosmology.

3.1. Hubble Parameter

This parameter sets the scale of our universe at present time. The present value of Hubble parameter is known as Hubble constant which lies in the range $H_0 = 65\text{--}75 \text{ km/s/Mpc}$. To find the expression of Hubble parameter for the underlying model under DGP braneworld gravity, first we differentiate Equation (5) w.r.t cosmic time t , which gives the following expression

$$\dot{H} = \frac{\dot{\rho}_\theta + \dot{\rho}_m}{3(2 - \Omega_B)}, \quad (10)$$

for Hubble horizon as IR cutoff, the expression of Hubble parameter is obtain by using Equations (2) and (7)–(10) as follows

$$\dot{H} = \frac{9(d^2 - 1)H_0^2\Omega_{m0}a^{3(d^2-1)}}{6 - 3\Omega_B - C(2 - \Delta)H^{-\Delta}}, \quad (11)$$

where $\Omega_{m0} = \frac{\rho_{m0}}{3H_0^2}$.

Next, we convert Equation (11) into redshift parameter z by using expression $dt = -\frac{dz}{H(z)(1+z)}$ and draw the plot of this expression in Figure 1 for different choices of d and Δ . We consider the best-fit values of model parameters $H_0 = 74$, $\Omega_{m0} = 0.32$, $C = 3$, $\Omega_{rc} = 0.0003$ and $\epsilon = -1$. From Figure 1, it is obvious that the range of H lies in the interval 95^{+35}_{-35} for selected range of redshift parameter which favors the recent observational data [73]. Again, in case of event horizon as IR cutoff, Hubble parameter becomes

$$\dot{H} = \frac{1}{(2 - \Omega_B)} \left(3H_0\Omega_{m0}(d^2 - 1)a^{3(d^2-1)} + (\Delta - 2)H\Omega_\theta \left(H - \left(\frac{3H^2\Omega_\theta}{C} \right)^{-\frac{1}{\Delta-2}} \right) \right). \quad (12)$$

In Figure 2, the Hubble parameter H has been plotted in term of redshift parameter z for different values of d and Δ . We also choose $H_0 = 74$, $\Omega_{m0} = 0.32$, $C = 3$, $\Omega_{rc} = 0.0003$ and $\epsilon = -1$. For the selected range of the redshift parameter, we obtain the interval of H , that lies in 97^{+23}_{-23} which is also consistent with recent observational data [73].

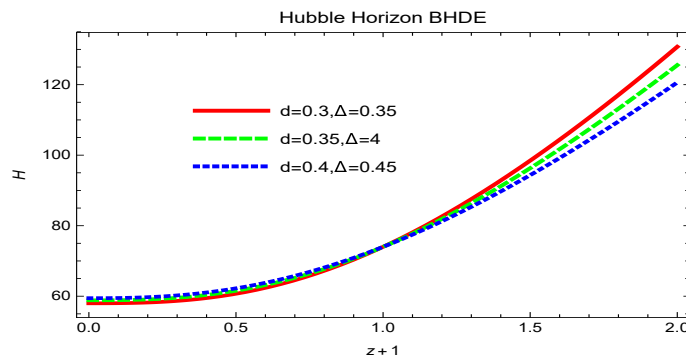


Figure 1. Estimation of Hubble parameter H versus redshift parameter $1 + z$ for interaction BHDE model with Hubble horizon in case of GDP braneworld cosmology.

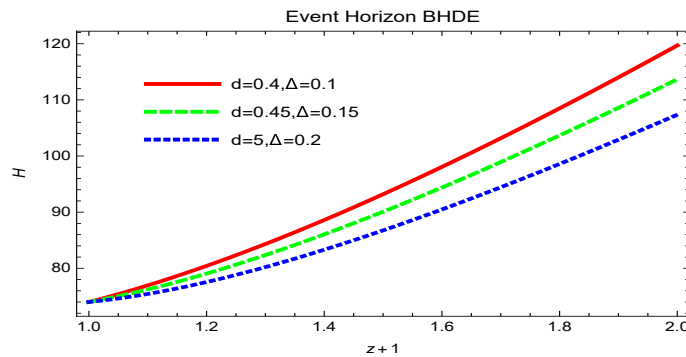


Figure 2. Plot of Hubble parameter H versus redshift parameter $1 + z$ for BHDE model with event horizon for GDP braneworld cosmology.

3.2. Equation of State Parameter

This parameter presents the ratio between pressure to the density of DE ($\omega_\theta = \frac{p_\theta}{\rho_\theta}$), also governs the rate at which the DE density evolves. See Table 1 below.

Table 1. The different phases of equation of state (EoS) parameter.

Decelerated Phase	$\omega_\theta = 1$	Stiff Fluid
	$\omega_\theta = \frac{1}{3}$	Radiation-Dominated
	$\omega_\theta = 0$	Dust Matter-Dominated
Accelerated Phase	$-1 < \omega_\theta < -\frac{1}{3}$	Quintessence
	$\omega_\theta = -1$	Cosmological Constant
	$\omega_\theta < -1$	Phantom-Dominated Era

For Hubble horizon, the expression of EoS parameter for underlying model can be obtain by using Equations (2) and (7) in term of redshift parameter, as follows

$$\omega_\theta = -1 - \frac{3H_0^2\Omega_{m0}d^2(1+z)^{-3(d^2-1)}}{CH^{2-\Delta}} - \frac{2-\Delta}{3H^2}\dot{H}. \quad (13)$$

In Figure 3, we show the evolution of EoS ω_θ versus z (redshift parameter) for some rational values of interaction parameter d and quantum deformation parameter Δ . For all these values of d and Δ , the EoS parameter remains in phantom dominated era ($\omega_\theta < -1$). In any case, for $d = 0.3$ and $\Delta = 0.35$ (red-line) the trajectory corresponds to quintessence era. It is also interesting to mention here that the trajectories also approach to a cosmological

constant Λ as $\omega_\vartheta \rightarrow -1$ in future epoch ($z < 1$). Similarly, in case of event horizon, the EoS parameter becomes

$$\omega_\vartheta = -1 - \frac{H_0^2 \Omega_{m0} d^2 (1+z)^{-3(d^2-1)}}{H^2 \Omega_\vartheta} - \frac{\Delta-2}{3H} \left(H - \left(\frac{3H^2 \Omega_\vartheta}{C} \right)^{-\frac{1}{\Delta-2}} \right). \quad (14)$$

The graphical behavior of ω_ϑ versus z is shown in Figure 4 for different values of d and Δ . We notice here that the EoS parameter, in the case of the BHDE model, remains in the phantom era, but for $d = 0.25$ and $\Delta = 0.02$, it approaches to a cosmological constant as well as quintessence behavior.

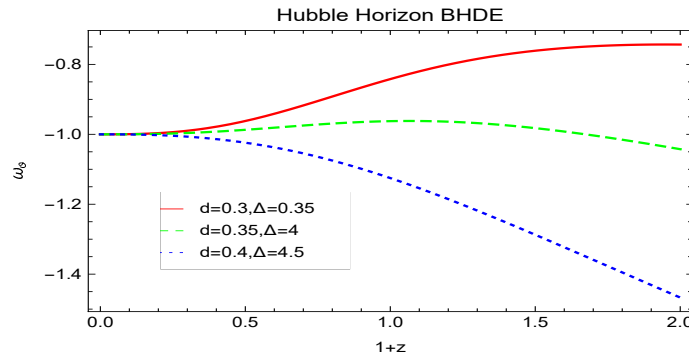


Figure 3. The EoS parameter ω_ϑ versus redshift parameter $1+z$ for interaction BHDE model with Hubble horizon for GDP braneworld cosmology.

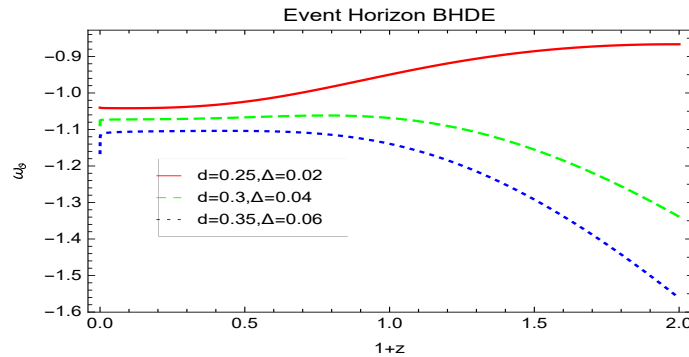


Figure 4. Plot of EoS parameter H versus redshift parameter $1+z$ for interaction BHDE model with event horizon for GDP braneworld cosmology.

3.3. Deceleration Parameter

The deceleration parameter q calculates the expansion history of the universe. The positive and negative sign of this parameter is to identify the decelerated and accelerated phases of the universe. If $-1 \leq q < 0$, it leads to accelerated phase while the decelerated phase is observed when $q \geq 0$. The mathematical expression of q is defined as

$$q = -\frac{a(t)\ddot{a}(t)}{(\dot{a}(t))^2} = -1 - \frac{\dot{H}}{H^2}. \quad (15)$$

In the case of the Hubble horizon, the expression of q for underlying model can be obtain by using Equations (5) and (11), as

$$q = -1 - \frac{9(d^2-1)H_0^2 \Omega_{m0} (1+z)^{-3(d^2-1)}}{H^2 (6-3\Omega_B - C(2-\Delta)H^{-\Delta})}. \quad (16)$$

The plot of the deceleration parameter against the redshift function is shown in Figure 5. We conclude that for the selected range of z , the deceleration parameter is

decreasing and decreases to more negative values. This range of q demonstrates the accelerating expansion of the universe for $z < 1.78$. Moreover, in case of event horizon, deceleration parameter becomes

$$q = -1 - \frac{1}{H^2(2 - \Omega_B)} \left(3H_0 H \Omega_{m0} (d^2 - 1) (1 + z)^{-3(d^2-1)} - (\Delta - 2) H^2 \Omega_\theta \left(\left(\frac{3H^2 \Omega_\theta}{C} \right)^{-\frac{1}{\Delta-2}} - H \right) \right). \quad (17)$$

The evolutionary behavior of the q (deceleration parameter) is plotted (Figure 6) for the BHDE model versus z (redshift function) for the same previous values of all parameters. From Figure 6, it is clear that the universe enters from an early deceleration phase to the current acceleration phase, which shows the compatibility with the observational data.

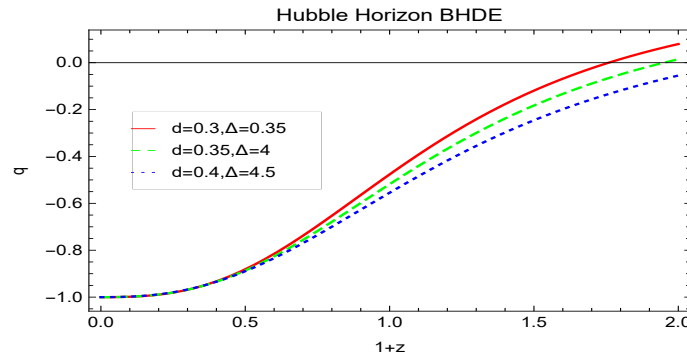


Figure 5. The evolutionary behavior deceleration parameter q versus redshift parameter $1 + z$ for interaction BHDE model with Hubble horizon for GDP braneworld cosmology.

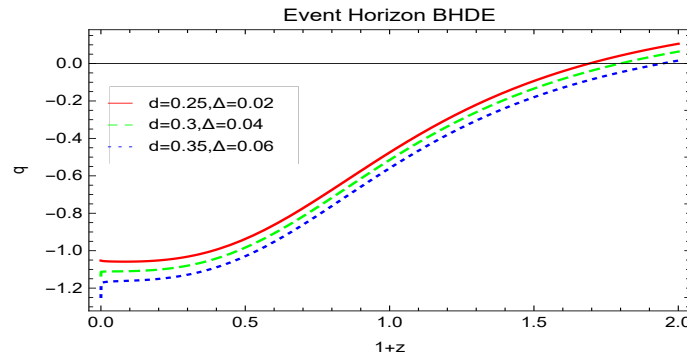


Figure 6. Plot of q versus $1 + z$ for BHDE model with event horizon for GDP braneworld cosmology.

3.4. Squared Speed of Sound Parameter

The squared speed of sound V_s^2 is an important tool to check the stability of any model. If $V_s^2 > 0$, it corresponds to the stability of model while $V_s^2 \leq 0$ leads to instability [74]. This parameter is defined as

$$V_s^2 = \frac{p'_\theta}{\rho'_\theta} = \frac{\dot{p}_\theta}{\dot{\rho}_\theta}. \quad (18)$$

Now, substitute $p_\theta = \rho_\theta \omega_\theta$ and differentiate it w.r.t to t , it becomes

$$V_s^2 = \frac{\dot{\omega}_\theta \rho_\theta}{\dot{\rho}_\theta} + \omega_\theta, \quad (19)$$

for Hubble horizon, Using Equations (11) and (13) one can obtain the expression of V_s^2 as follows

$$V_s^2 = -1 - \frac{3H_0^2 \Omega_{m0} d^2 (1 + z)^{-3(d^2-1)}}{c H^{2-\Delta}} - \frac{2 - \Delta}{3H^2} \dot{H} + \frac{H \dot{\omega}}{(2 - \Delta) \dot{H}}. \quad (20)$$

For different values of d and Δ , the squared speed of sound v_s^2 represented by Equation (20), is plotted in Figure 7 against redshift parameter z . The figure depicts the positive range of V_s^2 that corresponds to the stability of the BHDE model. In addition, for event horizon, this parameter yields

$$V_s^2 = -1 - \frac{H_0^2 \Omega_{m0} d^2 (1+z)^{-3(d^2-1)}}{H^2 \Omega_\theta} - \frac{\Delta-2}{3H} \left(H - \left(\frac{3H^2 \Omega_\theta}{C} \right)^{-\frac{1}{\Delta-2}} \right) - \left(\left(\frac{3H^2 \Omega_\theta}{C} \right)^{-\frac{1}{\Delta-2}} - H \right)^{-1} \frac{\dot{\omega}}{\Delta-2}. \quad (21)$$

The evolution of V_s^2 versus redshift parameter z for event horizon is shown in Figure 8. For this case, the trajectories of the squared speed of sound are shown $V_s^2 > 0$ only when $z \leq 1.2$ which leads to stability of the underlying model.

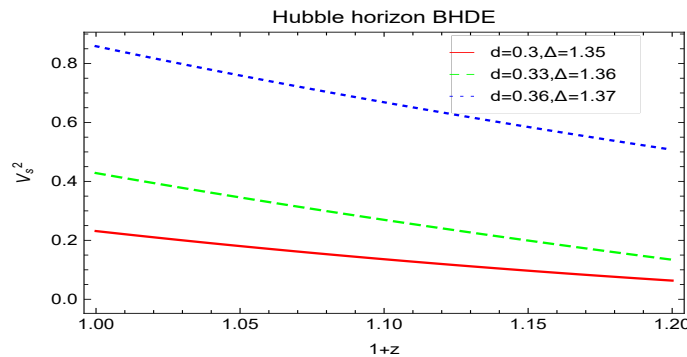


Figure 7. Plot of squared speed of sound V_s^2 versus redshift parameter $1+z$ for BHDE model with Hubble horizon for GDP braneworld cosmology.

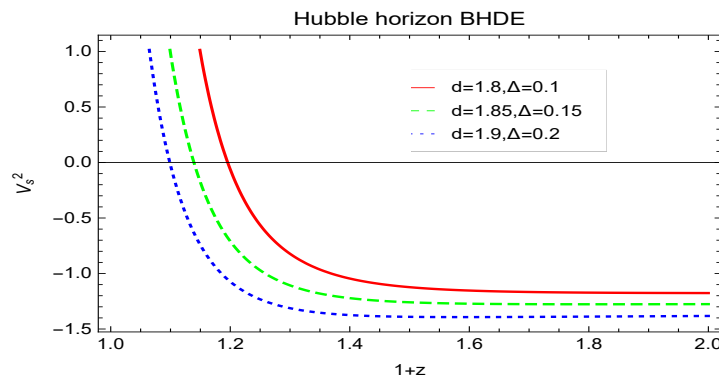


Figure 8. The V_s^2 as the function of z for interaction BHDE model with event horizon for GDP braneworld cosmology.

4. Cosmological Planes

In this section, we study the physical significance of $\omega_\theta - \omega'_\theta$ and state-finder planes for the BHDE model under DGP braneworld gravity.

4.1. $\omega_\theta - \omega'_\theta$ Plane

The $\omega_\theta - \omega'_\theta$ (where ' expresses the derivative w.r.t $\ln a$) plane analysis, is a very significant tool as it has been used to differentiate different DE models through trajectories on its plane. Initially, Caldwell and Linder [75] introduced this plane to investigate the behavior of the quintessence DE model. They divide this plane into two classes named thawing region where $\omega'_\theta > 0$ for $\omega_\theta < 0$ and the freezing region where $\omega'_\theta < 0$ for $\omega_\theta < 0$. It is interesting to mention here that cosmic expansion in the freezing phase is accelerating more compared to the thawing region. Now, one can differentiate Equation (13) w.r.t $\ln a$ to find the expression of ω'_θ for Hubble horizon as follows

$$\begin{aligned}
\omega'_\theta &= \frac{3H_0^2\Omega_{m0}(1+z)^{(3-3d^2)}}{CH^3(C(\Delta-2)H^{-\Delta}-3\Omega_B+6)^2} \left(-3C^2(d^2-1)(\Delta-2)^2H^{1-\Delta} + C^2(\Delta-2)^3 \right. \\
&\times (1+z)H^{-\Delta}\dot{H} - 6C(\Delta-2)(1+z)(d^2(\Delta-1)-1)(\Omega_B-2)\dot{H} + 3C(d^2-1)(\Delta-2) \\
&\times H \left(3(d^2+1)(\Omega_B-2) - (1+z)\dot{\Omega}_B \right) + 9d^2(\Delta-2)(1+z)(\Omega_B-2)^2H^\Delta\dot{H} - 27d^2(d^2 \right. \\
&\left. - 1)(\Omega_B-2)^2H^{\Delta+1} \right). \tag{22}
\end{aligned}$$

The plot of ω_θ versus ω'_θ is shown in Figure 9, where the horizontal axis is defined by ω_θ while the vertical axis presented by ω'_θ . From Figure 9, it is clear that $\omega'_\theta < 0$ as $\omega_\theta < 0$, which corresponds to the freezing phase. In case of event horizon, the expression of ω'_θ takes the following form

$$\begin{aligned}
\omega'_\theta &= \frac{3^{\frac{1}{2-\Delta}-1}(1+z)}{H^2((1+z)^{3d^2}H^2(\Omega_B-1)+H_0^2\Omega_{m0}(1+z)^3)} \left(- (H_0^2\Omega_{m0}(1+z)^{(3-3d^2)} + H^2(\Omega_B \right. \\
&- 1))C^{-1} \right)^{\frac{1}{2-\Delta}} \left(H_0^2\Omega_{m0}(1+z)^2((\Delta-2)(1+z)\dot{H} - 3(d^2-1)H) + (1+z)^{3d^2}H^2(\Delta \right. \\
&\times (\Omega_B-1)\dot{H} + H\dot{\Omega}_B) \left. \right) + \left(d^2H_0^2\Omega_{m0}(1+z)^{(3d^2+3)}H((\Omega_B-1)(3(d^2-1)H + 2(1 \right. \\
&+ z)\dot{H}) + (1+z)H\dot{\Omega}_B) \right) \left((1+z)^{3d^2}H^2(\Omega_B-1) + H_0^2\Omega_{m0}(1+z)^3 \right)^{-2}. \tag{23}
\end{aligned}$$

Using Equation (23), we plot Figure 10 (ω_θ vs. ω'_θ) for BHDE model. We note that $\omega'_\theta > 0$ for $\omega_\theta < 0$ which leads to the thawing region.

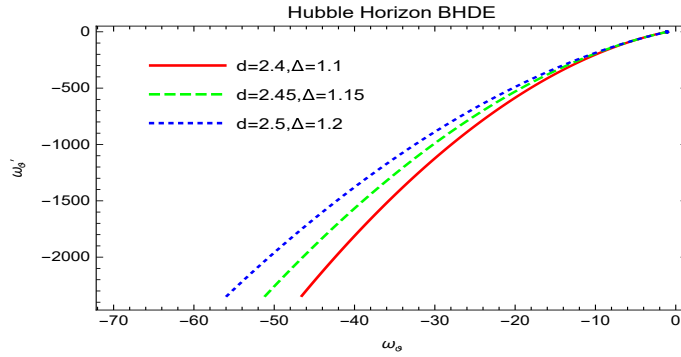


Figure 9. The behavior of ω_θ versus ω'_θ for interaction BHDE model with Hubble horizon in the context of GDP braneworld cosmology.

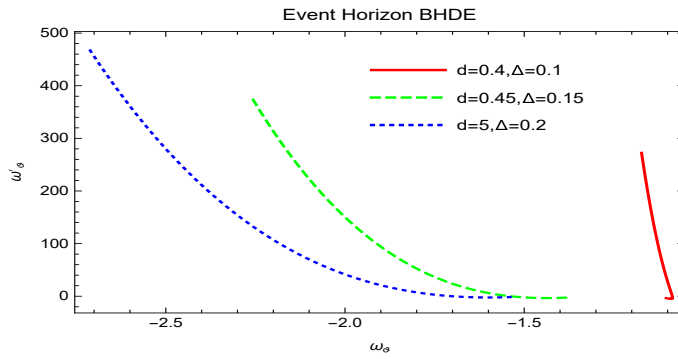


Figure 10. Plot of ω_θ versus ω'_θ for interaction BHDE model with event horizon in the framework of GDP braneworld cosmology.

4.2. Statefinder Diagnosis

The Hubble parameter and deceleration parameter are two traditional geometrical diagnostics that are known as the best choice to describe the cosmic expansion of the universe, but they cannot differentiate different DE models. Hence, Sahni et al. [76] introduced the statefinder $\{r, s\}$ plane with the help of two dimensionless parameters r and s , which not only characterized the different DE models uniquely but also depend upon H and q . Thus, with the help of $\{r, s\}$ plane, we can find the distance of underlying BHDE model from Λ CDM scenario. See Table 2 below.

Table 2. The different DE models corresponding to different values of r and s .

Model	r	s
Λ CDM	1	0
CDM limit	1	1
Phantom and Quintessence	<1	>0
Chaplygin Gas	>1	<0

The statefinder parameters in term of H and q is defined as

$$r = 1 + \frac{3\dot{H}}{H^2} + \frac{\dot{H}}{H^3}, \quad s = \frac{r-1}{3(q-\frac{1}{2})}. \quad (24)$$

Now, for the Hubble horizon, we calculate r and s for BHDE model under the DGP braneworld gravity, which obtained as

$$\begin{aligned} r &= 1 + \frac{27(d^2-1)H_0^2\Omega_{m0}(1+z)^{-3(d^2-1)}}{H^2(6-3\Omega_B-C(2-\Delta)H^{-\Delta})} + \frac{1}{H^3} \left(C(\Delta-2) - 3H^\Delta(-2+\Omega_B) \right)^{-2} \left(9(d^2-1)H_0^2\Omega_{m0}(1+z)^{(2-3d^2)}H^{\Delta-1} \left(C(\Delta-2)\left(\Delta(1+z)\dot{H}-3(d^2-1)H\right) + 3H^{\Delta+1}(3(d^2-1)(\Omega_B-2)+(1+z)\dot{\Omega}_B) \right) \right). \end{aligned} \quad (25)$$

$$\begin{aligned} s &= \frac{2}{3(2q-1)} \left(\frac{27(d^2-1)H_0^2\Omega_{m0}(1+z)^{-3(d^2-1)}}{H^2(6-3\Omega_B-C(2-\Delta)H^{-\Delta})} + \frac{1}{H^3} \left(C(\Delta-2) - 3H^\Delta(-2+\Omega_B) \right)^{-2} \times \left(9(d^2-1)H_0^2\Omega_{m0}(1+z)^{(2-3d^2)}H^{\Delta-1} \left(C(\Delta-2)\left(\Delta(1+z)\dot{H}-3(d^2-1)H\right) + 3H^{\Delta+1}(3(d^2-1)(\Omega_B-2)+(1+z)\dot{\Omega}_B) \right) \right) \right). \end{aligned} \quad (26)$$

The plot of r versus s in statefinder plane is shown in Figure 11. From Figure 11, we can see that the plot corresponds to Λ CDM model as we obtain $\{r, s\} = \{1, 0\}$. Furthermore, this figure shows that $r > 1$ and $s < 0$ which states the Chaplygin gas. Similarly, for event horizon, one can find the expressions of r and s .

The variations of the statefinder parameters is shown in Figure 12 for different values of d and Δ . Clearly, we see that $r > 0$ and $s < 0$ which again shows the Chaplygin gas. However, $r = 1$ and $s = 0$ leads to Λ CDM model.

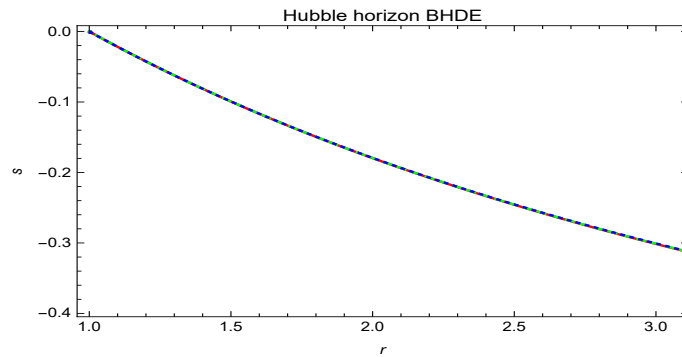


Figure 11. Variation of parameter r versus s for interaction BHDE model with Hubble horizon in the context of GDP braneworld cosmology.

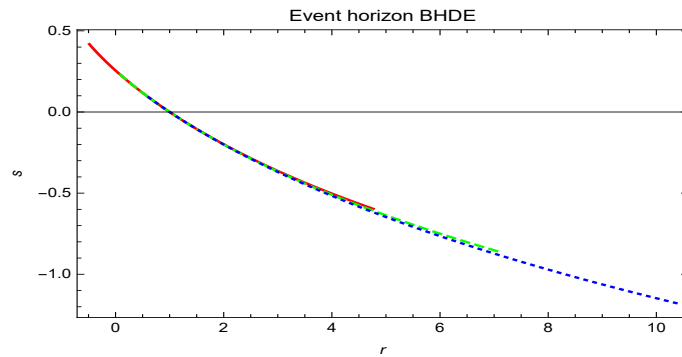


Figure 12. Plot of r versus s for interaction BHDE model with event horizon under GDP braneworld cosmology.

5. Generalized Second Law of Thermodynamics

Well-known relations between BH physics and thermodynamical laws provided us some useful information that BH emits thermal radiation (Hawking radiation). This connection motivated the exploration of the relation between gravity and thermodynamics. Initially, Jacobson [77] used fundamental relation between heat Q , entropy S and temperature T , $\delta Q = T\delta S$ (Clausius relation) with the proportionality of horizon area to entropy and derived the Einstein equation. Then, Padmanabhan [78] applied thermodynamics laws on the horizon and developed a general formalism in spherically symmetric space-times. Furthermore, this mechanism extended in the cosmological background by using the Hubble horizon. Cai and Kim [79] considered $T_A = \frac{1}{2\pi R_A}$ (Hawking temperature) and $S_A = \frac{\pi R_A^2}{G}$ (Bekenstein entropy) with the apparent horizon for a FRW universe and constructed the Friedmann equation in term of the first law of thermodynamics. This remarkable attempt (thermodynamical interpretation of gravity) opened a new horizon to investigate cosmological properties in terms of thermodynamics. In [80–82], authors established the relation between gravity and the higher-dimensional theories (Gauss–Bonnet term and Lovelock gravity). In general, the modified second thermodynamic law is known as the sum of the comic derivative among all horizon-related entropies and the normal entropy must be non-negative, i.e., $\dot{S}_{tot} = \dot{S} + \dot{S}_h \geq 0$, where S is the internal entropy of

the universe and S_h represents the Hawking entropy or horizon entropy. The first law of thermodynamics is defined as

$$TdS = dE + p_\vartheta dV \Rightarrow T\dot{S} = \dot{E} + p_\vartheta \dot{V}, \quad (27)$$

where $V = \frac{4\pi R_h^3}{3}$, $T_h = \frac{1}{2\pi R_h}$, $E = \frac{4\pi R_h^3}{3}(\rho_\vartheta + \rho_m)$ and $p_\vartheta = \omega_\vartheta \rho_\vartheta$. The total entropy is of the following form

$$\dot{S}_{tot} = \dot{S} + \dot{S}_h, \quad (28)$$

where \dot{S}_h is the external (horizon) entropy. In this paper, we consider Barrow entropy used in Equation (1) as horizon entropy. Therefore, the expression of total entropy in case of Hubble horizon as follows

$$\begin{aligned} S'_{tot} &= \frac{-16\pi^2}{3(1+z)H^6} \left(C(2-\Delta)\dot{H}H^{2-\Delta} + 9H_0^2\Omega_{m0}(d^2-1)(1+z)^{-3(d^2-1)}H^2 - 9H_0^2\Omega_{m0}\dot{H} \right. \\ &\times \left. (1+z)^{-3(d^2-1)} - 3C\dot{H}H^{2-\Delta} - CH^{-1-\Delta}\dot{H}\omega_\vartheta \right) + \frac{\gamma(\Delta+2)}{(1+z)H^{4+\Delta}}\dot{H}, \end{aligned} \quad (29)$$

where $\gamma = (\frac{4\pi}{A_0})^{\frac{\Delta+2}{2}}$.

Figure 13 presents the plot of total entropy vs. redshift parameter. We found the validity of GSLT as $S'_{tot} \geq 0$. Finally, for event horizon, the expression of S'_{tot} becomes

$$\begin{aligned} S'_{tot} &= \frac{-16\pi^2}{H(1+z)} \left(\frac{3H^2\Omega_\vartheta}{C} \right) \left(3H_0^2\Omega_{m0}(d^2-1)(1+z)^{-3(d^2-1)} + \left(H - \left(\frac{3H^2\Omega_\vartheta}{C} \right)^{-\frac{1}{\Delta-2}} \right) \right. \\ &\times \left. H^2(\Delta + \Omega_\vartheta) + 3H_0^2\Omega_{m0}(1+z)^{-3(d^2-1)} + 3H^2\Omega_\vartheta\omega_\vartheta \right) - \frac{\gamma(\Delta+2)}{(1+z)H} \left(\frac{3H^2\Omega_\vartheta}{C} \right)^{\frac{\Delta+1}{\Delta-2}} \left(H - \left(\frac{3H^2\Omega_\vartheta}{C} \right)^{-\frac{1}{\Delta-2}} \right). \end{aligned} \quad (30)$$

Figure 13 shows the plot of total entropy against the redshift parameter. From figure, it is clear that GSLT is also satisfied for the event horizon.

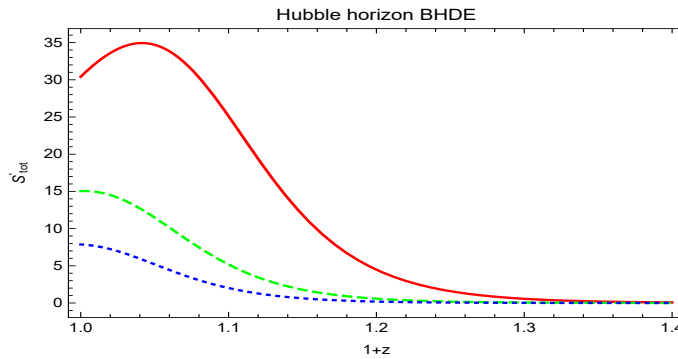


Figure 13. Plot of S'_{tot} versus redshift parameter $1+z$ for interaction interacting BHDE model with Hubble horizon under GDP braneworld cosmology.

6. Concluding Remarks

In this manuscript, we have made a versatile study on the interaction of the BHDE model in the context of GDP braneworld cosmology. The DGP braneworld is proposed by Giorgi Dvali, Gregory Gabadadze and Massimo Porrati for self-accelerating branch ($\epsilon = +1$) and normal branch ($\epsilon = -1$). We have tried to investigate various physical aspects of the newly proposed BHDE model under the normal branch of DGP cosmology. We have considered Γ as an interacting parameter between BHDE and pressureless DM.

In this scenario, we have assumed Hubble and event cutoffs to be the IR limit. In this framework, we addressed the nature of some important cosmological parameters such as Hubble H , EoS ω_θ , deceleration q and squared speed of sound V_s^2 . We have also investigated the nature of some cosmological planes such as $\omega_\theta - \omega'_\theta$ and the statefinder $\{r, s\}$. We have examined all these parameters and planes for different choices of d and Δ in the form of redshift. We have taken the best-fit values of all model parameters as $H_0 = 74$, $\Omega_{m0} = 0.32$, $C = 3$, $\Omega_{rc} = 0.0003$ and $\epsilon = -1$. Next, we are going to summarize the important results of our findings.

- We have examined the variation of Hubble parameter w.r.t redshift z in Figure 1 (Hubble horizon) and Figure 2 (event horizon). In Figure 1, we obtained the range of H lies in the interval 95^{+35}_{-35} which satisfied the recent observational data. Similarly, Figure 2 shows the range of Hubble parameter as $H = 97^{+23}_{-23}$ which again very near to observational limit.
- The EoS parameter ω_θ for the BHDE model is investigated in Figures 3 and 4 for Hubble and event cutoffs, respectively. From both figures, it is clear that $\omega_\theta < -1$ which shows that the universe is under the influence of the phantom dominated era. Both figures also remain in Λ CDM limit as $\omega_\theta \rightarrow -1$.
- Next, deceleration parameter is plotted with Hubble horizon (Figure 5) and event horizon (Figure 6) for BHDE model under braneworld cosmology. In Figure 5, we obtained $-1 \leq q < 0$ for selected range of redshift parameter, which corresponds to accelerated phase of the universe. In any case, at early epoch, when $z > 1.78$, the trajectories are shown to be in the decelerated phase. Moreover, in Figure 6 the graph of this parameter illustrated the decelerated phase $q \geq 0$ for $1.7 \leq z \leq 2$ while we obtain $-1 \leq q < 0$ for $0 \leq z < 1.7$ which leads to accelerated phase of the universe at present and future epoch.
- The graphical behavior of squared speed of sound parameter is found in Figures 7 and 8. We observed that the trajectories in both figures are shown $V_s^2 > 0$, which implies that the BHDE model under DGP braneworld gravity is stable for both cutoffs.
- We have also discussed $\omega_\theta - \omega'_\theta$ study for BHDE model in Figures 9 and 10. The trajectories of this plane in Figure 9 indicated the freezing phase as $\omega'_\theta < 0$ for $\omega_\theta < 0$ with Hubble horizon as IR cutoff. Similarly, Figure 10 examines the behavior of the same plane for event cutoff. From Figure, it is clear that $\omega'_\theta > 0$ for $\omega_\theta < 0$ which lead to thawing region. Therefore, cosmic expansion is more accelerating is observed for Hubble horizon.
- We analyzed the evolutionary behavior of statefinder plane in Figures 11 and 12. First of all, both figures correspond to Λ CDM model as $\{r = 1, s = 0\}$. Next, in both figures $\{r > 1, s < 0\}$ which lead to Chaplygin gas model.
- Finally, we examined the validity of GSLT through the evolution of total entropy area S'_{tot} in Figures 13 and 14 for Hubble and event cutoffs, respectively. In both cases, GSLT is valid as we found non-negative constraints ($S'_{tot} \geq 0$).

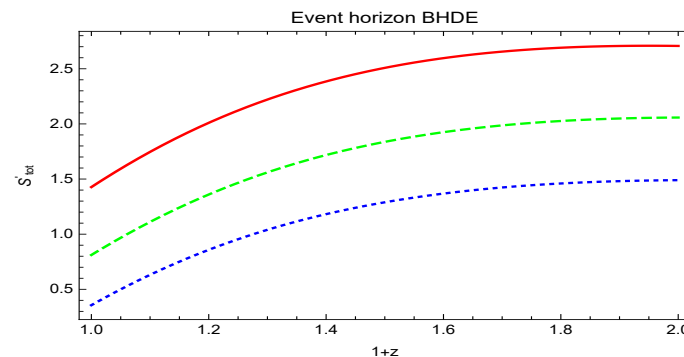


Figure 14. The evolution of S'_{tot} versus redshift parameter $1 + z$ for interacting BHDE model with event horizon under GDP braneworld cosmology.

As a final comment, we can conclude that all results for the BHDE model with Hubble and event cutoffs are stable and consistent with observational data. See Tables 3 and 4.

Table 3. Summary of the observational data on ω_{DE} .

ω_{DE}	Observational Schemes	References
$-1.56^{+0.60}_{-0.48}$	TT + lowE	[73]
$-1.58^{+0.52}_{-0.41}$	TT,TE,EE + lowE	[73]
$-1.57^{+0.50}_{-0.40}$	TT,TE,EE,lowE + lensing	[73]
$-1.04^{+0.10}_{-0.10}$	TT,TE,EE + lowE + lensing + BAO	[73]

Table 4. Summary of the observational data on q_0 .

q_0	Observational Schemes	References
-0.644 ± 0.223	BAO + Masers + TDSL + Pantheon	[83]
-0.6401 ± 0.187	BAO + Masers + TDSL + Pantheon + H_0	[83]
-0.930 ± 0.218	BAO + Masers + TDSL + Pantheon + $H(z)$	[83]
-1.2037 ± 0.175	BAO + Masers + TDSL + Pantheon + $H_0 + H(z)$	[83]

Author Contributions: The authors contributed equally to this work. Both authors have read and agreed to the published version of the manuscript.

Funding: This research received no external funding.

Conflicts of Interest: The authors declare no conflict of interest.

References

- Riess, A.G.; Filippenko, A.V.; Challis, P.; Clocchiatti, A.; Diercks, A.; Garnavich, P.M.; Gilliland, R.L.; Hogan, C.J.; Jha, S.; Kirshner, R.P.; et al. Observational Evidence from Supernovae for an Accelerating Universe and a Cosmological Constant. *Astron. J.* **1998**, *116*, 1009. [[CrossRef](#)]
- Perlmutter, S.; Aldering, G.; Aldering, G.; Knop, R.A.; Nugent, P.; Castro, P.G.; Deustua, S.; Fabbro, S.; Goobar, A.; Groom, D.E.; Hook, I.M.; et al. Measurements of Ω and Λ from 42 High-Redshift Supernovae. *Astrophys. J.* **1999**, *517*, 565. [[CrossRef](#)]
- Contaldi, C.R.; Hoekstra, H.; Lewis, A. Joint Cosmic Microwave Background and Weak Lensing Analysis: Constraints on Cosmological Parameters. *Phys. Rev. Lett.* **2003**, *90*, 221303. [[CrossRef](#)] [[PubMed](#)]
- Spergel, D.N.; Verde, L.; Peiris, H.V.; Komatsu, E.; Nolta, M.R.; Bennett, C.L.; Halpern, M.; Hinshaw, G.; Jarosik, N.; Kogut, A.; et al. First-Year Wilkinson Microwave Anisotropy Probe (WMAP)* Observations: Determination of Cosmological Parameters. *Astrophys. J. Suppl. Ser.* **2003**, *148*, 175. [[CrossRef](#)]
- Spergel, D.N.; Bean, R.; Doré, O.; Nolta, M.R.; Bennett, C.L.; Dunkley, J.; Hinshaw, G.; Jarosik, H.; Komatsu, E.; Page, L.; et al. Wilkinson Microwave Anisotropy Probe (WMAP) Three Year Results: Implications for Cosmology. *Astrophys. J. Suppl.* **2007**, *170*, 377. [[CrossRef](#)]
- Eisenstein, D.J.; Zehavi, I.; Hogg, D.W.; Scoccimarro, R.; Blanton, M.R.; Nichol, R.C.; Scranton, R.; Seo, H.-J.; Tegmark, M.; Zheng, Z.; et al. Detection of the Baryon Acoustic Peak in the Large-Scale Correlation Function of SDSS Luminous Red Galaxies. *Astrophys. J.* **2005**, *633*, 560. [[CrossRef](#)]
- Percival, W.J.; Reid, B.A.; Eisenstein, D.J.; Bahcall, N.A.; Budavari, T.; Frieman, J.A.; Fukugita, M.; Gunn, J.E.; Ivezić, Ž.; Knapp, G.R.; et al. Baryon acoustic oscillations in the Sloan Digital Sky Survey Data Release 7 galaxy sample. *Mon. Not. Roy. Astron. Soc.* **2010**, *401*, 2148–2168. [[CrossRef](#)]
- Sahni, V.; Starobinsky, A.A. THE CASE FOR A POSITIVE COSMOLOGICAL Λ -TERM. *Int. J. Mod. Phys. D* **2000**, *9*, 373–443. [[CrossRef](#)]
- Weinberg, S. The cosmological constant problem. *Rev. Mod. Phys.* **1989**, *61*, 1–23. [[CrossRef](#)]
- Bamba, K.; Capozziello, S.; Nojiri, S.; Odintsov, S.D. Dark energy cosmology: The equivalent description via different theoretical models and cosmography tests. *Astrophys. Space Sci.* **2012**, *342*, 155–228. [[CrossRef](#)]
- Bamba, K.; Myrzakulov, R.; Nojiri, S.; Odintsov, S.D. Reconstruction of $f(T)$ gravity: Rip cosmology, finite-time future singularities, and thermodynamics. *Phys. Rev. D* **2012**, *85*, 104036. [[CrossRef](#)]
- Bamba, K.; Geng, C.Q.; Lee, C.C. Comment on “Einstein’s Other Gravity and the Acceleration of the Universe”. *arXiv* **2010**, arXiv:1008.4036.

13. Bamba, K.; Nojiri, S.; Odintsov, S.D. Trace-anomaly driven inflation in $f(T)$ gravity and in minimal massive bigravity. *Phys. Lett. B* **2014**, *731*, 257–264. [CrossRef]
14. Urban, F.R.; Zhitnitsky, A.R. The cosmological constant from the QCD Veneziano ghost. *Phys. Lett. B* **2010**, *688*, 9–12. [CrossRef]
15. Urban, F.R.; Zhitnitsky, A.R. Cosmological constant from the ghost: A toy model. *Phys. Rev. D* **2009**, *80*, 063001. [CrossRef]
16. García-Bellido, J.; Haugbølle, T. The radial BAO scale and Cosmic Shear, a new observable for Inhomogeneous Cosmologies. *J. Cosmol. Astropart. Phys.* **2009**, *0909*, 018. [CrossRef]
17. Alkalaev, K.; Grigoriev, M. Unified BRST description of AdS gauge fields. *Nucl. Phys. B* **2010**, *835*, 197–220. [CrossRef]
18. Ohta, N. Dark energy and QCD ghost. *Phys. Lett. B* **2011**, *695*, 41–44. [CrossRef]
19. Caldwell, R.R. A phantom menace? Cosmological consequences of a dark energy component with super-negative equation of state. *Phys. Lett. B* **2002**, *545*, 23–29. [CrossRef]
20. Nojiri, S.; Odintsov, S.D. de Sitter brane universe induced by phantom and quantum effects. *Phys. Lett. B* **2003**, *565*, 1–9. [CrossRef]
21. Nojiri, S.; Odintsov, S.D. Quantum de Sitter cosmology and phantom matter. *Phys. Lett. B* **2003**, *562*, 147–152. [CrossRef]
22. Chiba, T.; Okabe, T.; Yamaguchi, M. Kinetically driven quintessence. *Phys. Rev. D* **2000**, *62*, 023511. [CrossRef]
23. Armen-Picon, C.; Mukhanov, V.; Steinhardt, P.J. Dynamical Solution to the Problem of a Small Cosmological Constant and Late-Time Cosmic Acceleration. *Phys. Rev. Lett.* **2000**, *85*, 4438–4441. [CrossRef]
24. Damour, T.; Mukhanov, V. k-Inflation. *Phys. Lett. B* **1999**, *458*, 209–218.
25. Wei, H.; Cai, R.G. A new model of agegraphic dark energy. *Phys. Lett. B* **2008**, *660*, 113–117. [CrossRef]
26. Cai, R.G. A dark energy model characterized by the age of the Universe. *Phys. Lett. B* **2007**, *657*, 228–231. [CrossRef]
27. Hsu, S.D.H. Entropy Bounds and Dark Energy. *Phys. Lett. B* **2004**, *594*, 13–16. [CrossRef]
28. Li, M. A Model of Holographic Dark Energy. *Phys. Lett. B* **2004**, *603*, 1–5. [CrossRef]
29. De Felice, A.; Tsujikawa, S. f(R) Theories. *Living Rev. Rel.* **2010**, *13*, 3. [CrossRef] [PubMed]
30. Nojiri, S.; Odintsov, S.D. Unified cosmic history in modified gravity: From theory to Lorentz non-invariant models. *Phys. Rep.* **2011**, *505*, 59–144. [CrossRef]
31. Linder, E.V. Einstein’s other gravity and the acceleration of the Universe. *Phys. Rev. D* **2010**, *81*, 127301. [CrossRef]
32. Nojiri, S.; Odintsov, S.D. Modified Gauss–Bonnet theory as gravitational alternative for dark energy. *Phys. Lett. B* **2005**, *631*, 1–6. [CrossRef]
33. Cognola, G.; Elizalde, E.; Nojiri, S.; Odintsov, S.D.; Zerbini, S. Dark energy in modified Gauss–Bonnet gravity: Late-time acceleration and the hierarchy problem. *Phys. Rev. D* **2006**, *73*, 084007. [CrossRef]
34. Dvali, G.R.; Gabadadze, G.; Porrati, M. 4D gravity on a brane in 5D Minkowski space. *Phys. Lett. B* **2000**, *485*, 208–214. [CrossRef]
35. Deffayet, C. Cosmology on a brane in Minkowski bulk. *Phys. Lett. B* **2001**, *502*, 199–208. [CrossRef]
36. Deffayet, C.; Dvali, G. Accelerated universe from gravity leaking to extra dimensions. *Phys. Rev. D* **2002**, *65*, 044023. [CrossRef]
37. Mukherjee, A. Spherical collapse in DGP braneworld cosmology. *arXiv* **2020**, arXiv:2008.08979.
38. Koyama, K.; Maartens, R. Structure formation in the Dvali–Gabadadze–Porrati cosmological model. *J. Cosmol. Astropart. Phys.* **2006**, *01*, 016. [CrossRef]
39. Multamaki, T.; Gaztanaga, E.; Manera, M. Large-scale structure in non-standard cosmologies. *Mon. Not. R. Astron. Soc.* **2003**, *344*, 761–775. [CrossRef]
40. Cardoso, A.; Koyama, K.; Seahra, S.S.; Silva, F.P. Cosmological perturbations in the DGP braneworld: Numeric solution. *Phys. Rev. D* **2008**, *77*, 083512. [CrossRef]
41. Biswas, M.; Debnath, U.; Ghosh, S. Generalized ghost dark energy in DGP model. *Int. J. Geo. Meth. Mod. Phys.* **2019**, *16*, 1950178. [CrossRef]
42. Nojiri, S.; Odintsov, S.D.; Saridakis, E.N. Holographic inflation. *Phys. Lett. B* **2019**, *797*, 134829. [CrossRef]
43. Paul, T. Holographic correspondence of F(R) gravity with/without matter fields. *Europhys. Lett.* **2019**, *127*, 20004. [CrossRef]
44. Bargach, A.; Bargach, F.; Errahmani, A.; Ouali, T. Induced gravity effect on inflationary parameters in a holographic cosmology. *Int. J. Mod. Phys. D* **2020**, *29*, 2050010. [CrossRef]
45. Horvat, R. Holographic bounds and Higgs inflation. *Phys. Lett. B* **2011**, *699*, 174–176. [CrossRef]
46. Elizalde, E.; Timoshkin, A. Viscous fluid holographic inflation. *Eur. Phys. J. C* **2019**, *79*, 732. [CrossRef]
47. Oliveros, A.; Acero, M.A. Inflation driven by a holographic energy density. *Europhys. Lett.* **2019**, *128*, 59001. [CrossRef]
48. Gao, C.; Wu, F.; Chen, X.; Shen, Y.G. Holographic dark energy model from Ricci scalar curvature. *Phys. Rev. D* **2009**, *79*, 043511. [CrossRef]
49. Colgáin, E.Ó.; Jabbar, M.M.S. A Critique of Holographic Dark Energy. *arXiv* **2021**, arXiv:2102.09816.
50. Tsallis, C.; Cirto, L.J.L. Black hole thermodynamical entropy. *Eur. Phys. J. C* **2013**, *73*, 2487. [CrossRef]
51. Moradpour, H.; Moosavi, S.A.; Lobo, I.P.; Graça, J.P.M.; Jawad, A.; Salako, I.G. Thermodynamic approach to holographic dark energy and the Rényi entropy. *Eur. Phys. J. C* **2018**, *78*, 829. [CrossRef]
52. Dixit, A.; Bhardwaj, V.K.; Pradhan, A. RHDE models in FRW Universe with two IR cut-offs with redshift parametrization. *Eur. Phys. J. Plus* **2020**, *135*, 831. [CrossRef]
53. Sayahian-Jahromi, A.; Moosavi, S.A.; Moradpour, H.; Graça, J.P.M.; Lobo, I.P.; Salako, I.G.; Jawad, A. Generalized entropy formalism and a new holographic dark energy model. *Phys. Lett. B* **2018**, *780*, 21–24. [CrossRef]
54. Dubey, V.C.; Sharma, U.K.; Pradhan, A. Sharma–Mittal holographic dark energy model in conharmonically flat space-time. *Int. J. Geom. Methos. Mod. Phys.* **2021**, *18*, 2150002. [CrossRef]

55. Saridakis, E.N. Barrow holographic dark energy. *Phys. Rev. D* **2020**, *102*, 123525. [[CrossRef](#)]
56. Hawking, S.W. Black holes in general relativity. *Commun. Math. Phys.* **1972**, *25*, 152–166. [[CrossRef](#)]
57. Bekenstein, J.D. Generalized second law of thermodynamics in black-hole physics. *Phys. Rev. D* **1974**, *9*, 3292–3300. [[CrossRef](#)]
58. Kolmogorov, A.N. A new metric invariant of transitive dynamical systems and of automorphisms of Lebesgue spaces. *Dokl. Acad. Sci. USSR* **1958**, *119*, 861–864.
59. Tsallis, C. Black Hole Entropy: A Closer Look. *Entropy* **2020**, *22*, 17. [[CrossRef](#)] [[PubMed](#)]
60. Sharma, B.D.; Mittal, D.P. New non-additive measures of entropy for discrete probability distributions. *J. Math. Sci.* **1975**, *10*, 28–40.
61. Masi, M. A step beyond Tsallis and Renyi entropies. *Phys. Lett. A* **2005**, *383*, 217–224. [[CrossRef](#)]
62. Lesche, B. Instabilities of Rényi entropies. *J. Stat. Phys.* **1982**, *27*, 419–422. [[CrossRef](#)]
63. Barrow, J.D. The area of a rough black hole. *Phys. Lett. B* **2020**, *808*, 135643. [[CrossRef](#)]
64. Wang, B.; Gong, Y.; Abdalla, E. Thermodynamics of an accelerated expanding universe. *Phys. Rev. D* **2006**, *74*, 083520. [[CrossRef](#)]
65. Sadjadi, M.H.; Honardoost, M. Thermodynamics second law and $\omega = -1$ crossing(s) in interacting holographic dark energy model. *Phys. Lett. B* **2007**, *647*, 231–236. [[CrossRef](#)]
66. Arevalo, F.; Cifuentes, P.; Peña, F. Generalized Second Law of Thermodynamics for Holographic Dark Energy and cosmological interaction. *Astrophys. Space Sci.* **2016**, *361*, 45. [[CrossRef](#)]
67. Dixit, A.; Bharadwaj, V.K.; Pradhan, A. Barrow HDE model for Statefinder diagnostic in non-flat FRW universe. *arXiv* **2021**, arXiv:2103.08339.
68. Sharma, U.K.; Varshney, G.; Dubey, V.C. Barrow agegraphic dark energy. *Int. J. Mod. Phys. D* **2021**, *30*, 2150021. [[CrossRef](#)]
69. Srivastava, S.; Sharma, U.K. Barrow holographic dark energy with hubble horizon as IR cutoff. *Int. J. Geom. Methods Mod. Phys.* **2021**, *18*, 2150014. [[CrossRef](#)]
70. Mamon, A.A.; Paliathanasis, A.; Saha, S. Dynamics of an Interacting Barrow Holographic Dark Energy Model and its Thermodynamic Implications. *Eur. Phys. J. Plus* **2021**, *136*, 134. [[CrossRef](#)]
71. Bolotin, Y.L.; Kostenko, A.; Lemets, O.A.; Yerokhin, D.A. Cosmological evolution with interaction between dark energy and dark matter. *Int. J. Geom. Methos. Mod. Phys.* **2015**, *24*, 1530007. [[CrossRef](#)]
72. Sadri, E.; Khurshudyan, M.; Zeng, D.F. Scrutinizing Various Phenomenological Interactions In The Context Of Holographic Ricci Dark Energy Models. *arXiv* **2019**, arXiv:1904.11600.
73. Collaboration, P.; Aghanim, N.; Akrami, Y.; Ashdown, M.; Aumont, J.; Baccigalupi, C.; Ballardini, M.; Banday, A.J.; Barreiro, R.B.; Bartolo, N.; et al. Planck 2018 results. VI. Cosmological parameters. *arXiv* **2020**, arXiv:1807.0620.
74. Hawking, S.W.; Ellis, G.F.R. *The Large Scale Structure of Space-Time*; Cambridge University Press: Cambridge, UK, 1973.
75. Caldwell, R.R.; Linder, E.V. The Limits of Quintessence. *Phys. Rev. Lett.* **2005**, *95*, 141301. [[CrossRef](#)]
76. Sahni, V.; Saini, T.D.; Starobinsky, A.A.; Alam, U. Statefinder—A new geometrical diagnostic of dark energy. *J. Exp. Theor. Phys. Lett.* **2003**, *77*, 201. [[CrossRef](#)]
77. Jacobson, T. Thermodynamics of Spacetime: The Einstein Equation of State. *Phys. Rev. Lett.* **1995**, *75*, 1260–1263. [[CrossRef](#)] [[PubMed](#)]
78. Padmanabhan, T. Classical and Quantum Thermodynamics of horizons in spherically symmetric spacetimes. *Class. Quantum Grav.* **2002**, *19*, 5387–5408. [[CrossRef](#)]
79. Cai, R.G.; Kim, S.P. First Law of Thermodynamics and Friedmann Equations of Friedmann-Robertson-Walker Universe. *J. High Energy Phys.* **2005**, *02*, 050. [[CrossRef](#)]
80. Bamba, K.; Geng, C.Q.; Nojiri, S.; Odintsov, S.D. Equivalence of the modified gravity equation to the Clausius relation. *Europhys. Lett.* **2010**, *89*, 50003. [[CrossRef](#)]
81. Akbar, M.; Cai, R.G. Friedmann Equations of FRW Universe in Scalar-tensor Gravity, f(R) Gravity and First Law of Thermodynamics. *Phys. Lett. B* **2006**, *635*, 7–10. [[CrossRef](#)]
82. Lanczos, C. A Remarkable property of the Riemann-Christoffel tensor in four dimensions. *Ann. Math.* **1938**, *39*, 842–850.
83. Capozziello, S.; Ruchika, Sen, A.A. Model independent constraints on dark energy evolution from low-redshift observations. *Mon. Not. Roy. Astron. Soc.* **2019**, *484*, 4484–4494. [[CrossRef](#)]